THE JOURNAL OF PHYSICAL CHEMISTRY C

Article

pubs.acs.org/JPCC

Nature of Interaction between Semiconducting Nanostructures and Biomolecules: Chalcogenide QDs and BNNT with DNA Molecules

Zhoufei Wang,[†,‡] Haiying He,[*,§] William Slough,[†] Ravindra Pandey,[*,†] and Shashi P. Karna[*,∥]

[†]Michigan Technological University, Houghton, Michigan 49931, United States

[‡]South China Agricultural University, Guangzhou 510642, China

[§]Department of Physics and Astronomy, Valparaiso University, Valparaiso, Indiana 46383, United States

[∥]Weapons and Materials Research Directorate, ATTN: RDRL-WM, US Army Research Laboratory, Aberdeen Proving Ground, Maryland 21005-5069, United States

Supporting Information

ABSTRACT: Interactions of DNA oligomers with two categories of semiconducting nanostructures—chalcogenide quantum dots (QDs) and boron nitride nanotubes (BNNTs)—owing to their widespread presence in bio-inspired processes are investigated using the first-principles density functional theory and continuum solvent model. The chalcogenide QDs interact strongly at their metal centers featuring electrostatic interaction with DNA oligomers at oxygen or nitrogen site, while BNNTs form covalent bonds with DNA oligomers at multiple surface sites. It is found that the different bonding nature leads to distinctly different response to the aqueous environment; the presence of solvent drastically reduces the binding strength of nucleobases with the QDs due to the strong electrostatic screening. This is not the case with BNNTs for which the covalent bonding is barely affected by the solvent. This study thus clearly shows how a solvent medium influences chemical interactions providing guidance for technological applications of bioconjugated systems.

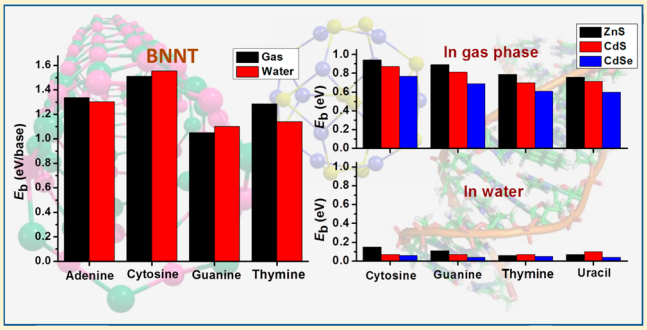

1. INTRODUCTION

The fusion of nanotechnology and biology has recently occurred at a rapid pace leading to increasing interface of nanostructured materials with biological molecules for the next-generation health-related applications. While these two systems are common in the size of their entities falling into the scale of subnano- and nanometers, they are drastically different in their chemical composition, bonding, and internal cohesion. The nanostructures are mostly composed of inorganic materials having covalent, ionic, or metallic bonds, while the biomolecules are mostly organic molecules primarily composed of C, H, O, and N forming strong covalent bonds, $\pi-\pi$ interaction, and H-bonds. With the existing great opportunity together with the great challenge, it is essential to understand the fundamental interaction between nanostructures and biomolecules at the atomic level in their working environment.

Since the nucleic acid bases are key components of the genetic macromolecules—deoxyribonucleic acid (DNA) and ribonucleic acid (RNA)—playing a central role in all biological systems, we consider the interaction between nucleobases or small fragments of DNA with a selection of important semiconducting nanostructures represented by the chalcogenide quantum dots (QDs) and boron nitride nanotubes (BNNTs). This study is the first step of our efforts toward a full-scale quantum mechanical investigation of DNA strands with nanostructures. Note that semiconducting QDs based on ZnS and CdS have been proposed as candidate materials for the photoelectrochemical label for biosensing events, luminescent labels for biorecognition events, and luminescent probes for DNA.[1−5] The sulfide-based quantum dots appear to have advantages over traditional fluorescent probes due to their broad absorption spectra, narrow emission spectra, and resistance to photobleaching.[2] In addition, their nonlinear refractive index and nonlinear optical absorption were estimated to be several orders of magnitude larger than those of the bulk materials.[5] There is, however, scarcity of study on the interaction between the semiconductor QDs and DNA molecules. As attractive as the ionic-bonding dominated chalcogenide QDs, the covalently bonded BNNTs[6,7] have become a very promising candidate in electronics,[8] drug delivery,[9] and other biomedical applications.[10−12] The study of the toxicity of these semiconducting nanotubes has just begun.[13] A recent study shows that BNNTs have no toxicity for cell lines but have positive effect on accelerated osteoblast differentiation and growth.[10] This was attributed to the strong affinity of protein to BNNTs. Zhi et al. reported strong

Received: August 19, 2015
Revised: October 27, 2015
Published: November 2, 2015

DOI: 10.1021/acs.jpcc.5b08084
J. Phys. Chem. C 2015, 119, 25965−25973

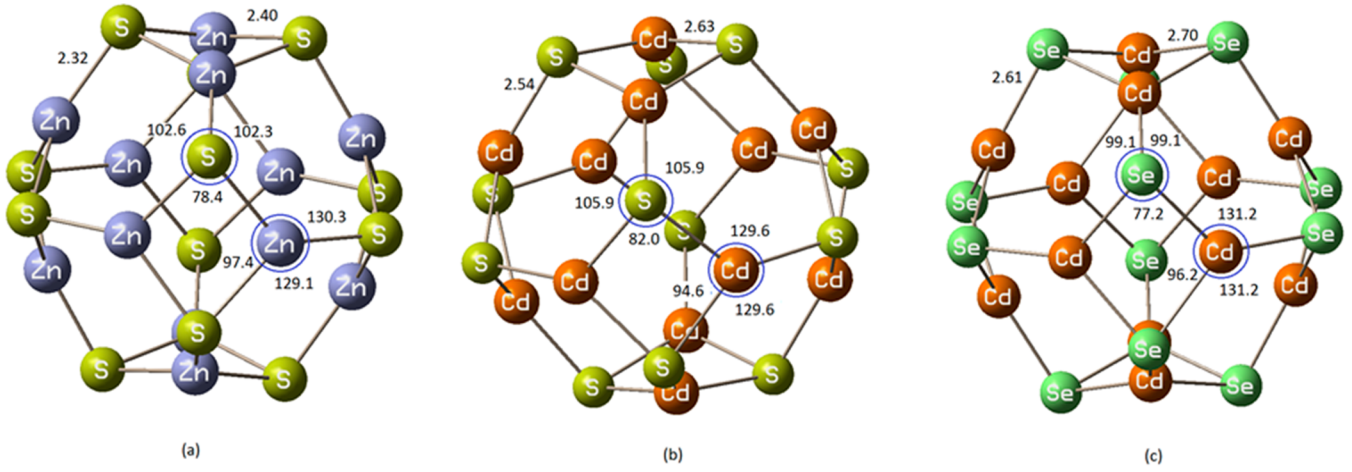

Figure 1. Calculated ground state configurations of (a) $(ZnS)_{12}$, (b) $(CdS)_{12}$, and (c) $(CdSe)_{12}$.

interaction and immobilization of ferritin protein on BNNT surfaces.[14] The dispersion and DNA-mediated assembly of BNNTs in solutions were reported.[15] Strong covalent interactions were also observed for BNNTs with organic polymers in forming composites.[16]

On the other hand, quantum mechanical studies have been reported for the interaction of DNA/RNA nucleobases with a variety of nanostructures, such as CNTs,[17] BNNTs,[18] BN sheets,[19] metallic clusters,[20,21] oxide nanoparticles,[22] and clays[23,24] showing a rich and diverse range of physics and chemistry involved in the interfacial interaction. The study of DNA interacting with chalcogenide QDs is still lacking. In addition, these previous computational studies are gas phase calculations with few exceptions. It is important to note that most relevant applications nonetheless occur in aqueous environment. Recent studies have revealed the importance of including the solvent effect for interactions in solutions.[25,26] We aim to investigate the solvent effect in these reactions. Although fully account of the thermal fluctuation and taking into account counterions may be a more faithful representation, the significantly more cost has limited its use in this study. It is not our current interest to extract the full wrapping picture of DNA around these nanostructures, but rather to look at the solvent effect toward the binding of DNA to QDs and BNNTs and compare their differences. More specifically, in the present study, we will calculate stable geometries, site specific interaction energies, electronic properties via molecular orbital analysis, and charge density distribution of the bioconjugated complexes. The insights gained from this comparison study can provide an in-depth understanding of the interaction of these low-dimensional semiconducting materials with biological molecules at the atomic level and pave the way for more realistic theoretical simulations of nano-bio interactions in aqueous solutions.

2. METHOD

The electronic structure calculations were performed in the framework of the density functional theory (DFT) using the Gaussian09 program package.[27] All calculations were considered to be converged when the force on each ion is less than 0.01 eV/Å with a convergence in the RMS density matrix to 10^{-8} and the total energy to 10^{-5} eV. The B3LYP functional form[28] and the LanL2DZ basis sets[29−31] were employed for calculations of chalcogenide QDs with DNA bases. Considering that the chemical bonding in the semiconducting QD is semi-ionic, our choice of the hybrid exchange and correlation functional form, B3LYP is expected to be reasonably accurate in describing site-specific interactions between nucleobases and QDs. Results of all-electron calculations using the 6-31G(d) Gaussian basis sets (Supporting Information Table S1) show a consistent difference of 0.1−0.2 eV in the binding energy. Inclusion of the dispersion[32] further increases the binding energy by ∼0.4 eV without changing the relative stability of different nucleobases obtained at the B3LYP-D2 level of theory. The hybrid density functional form wB97XD,[33] which includes empirical atom−atom dispersion corrections, was employed for BNNT interacting with DNA oligomers. This functional can also take proper account of the nonbonded interactions, including the van der Waals interactions. The 3-21G(d) basis sets were used for all the atoms of BNNT and DNA oligomers in our calculations. It has been shown that wB97X-D performs noticeably better relative to the other empirical dispersion-corrected density functional forms for covalent systems.[34]

The solvent effects were included via the polarizable continuum model (PCM) in which the polarization charge Q is scaled such that the total polarization charge obeys Gauss's law.[35] In this model, the water solvent is represented by a homogeneous continuum medium having a dielectric constant of 78.39, which is polarized by the solute placed in a cavity built in the bulk of water.

3. RESULTS AND DISCUSSION

Chalcogenide QDs and DNA Bases. We employ a finite cluster model to simulate semiconducting chalcogenides QDs in which QDs are represented by the subnanometer clusters, e.g., $(ZnS)_{12}$, $(CdS)_{12}$, and $(CdSe)_{12}$ which are highly symmetric, spherical cagelike, and stable (Figure 1). Their interactions with the nucleotide bases of DNA and RNA, namely adenine (A), cytosine (C), guanine (G), thymine (T), and uracil (U), are considered. The geometrical structure of the isolated nucleobases and the QD were optimized as a prior step to the nucleobase−QD complex calculations. Subsequently, total energy calculations of the complex with respect to the separation between the QD and the nucleobases were performed, yielding the energy surface describing the interaction of semiconducting QDs with the nucleobase.

The choice of cagelike highly symmetric chalcogenide QDs was based on the several previous studies[36−38] in which the 24-

DOI: 10.1021/acs.jpcc.5b08084
J. Phys. Chem. C 2015, 119, 25965−25973

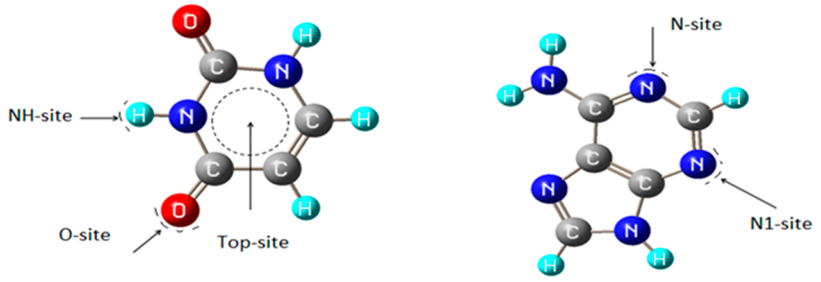

Figure 2. Different binding sites of uracil and adenine (C: gray; N: navy blue; H: light blue; O: red).

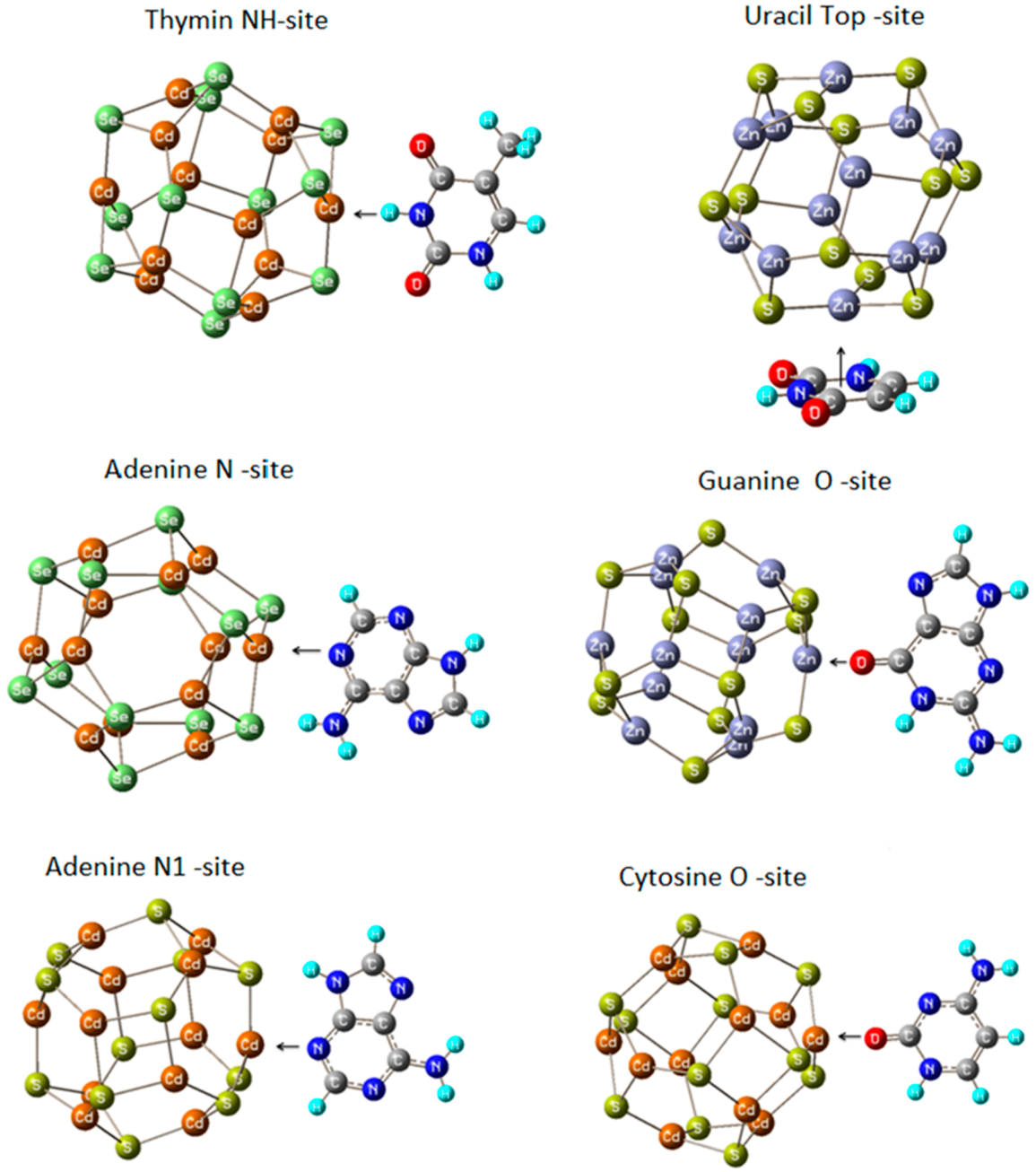

Figure 3. Samples of nucleobases approaching $(ZnS)_{12}$, $(CdS)_{12}$, or $(CdSe)_{12}$ nanoclusters from different binding sites to form bioconjugated complexes.

atom icosahedra-derived configuration was found to be stable and a prospective candidate for cluster assembly of materials. For a $(MX)_{12}$ (M = Zn, Cd; X = S, Se) QD, it is based on six $(MX)_2$ and eight $(MX)_3$ rings forming a truncated octahedron in which all M and X vertices remain equivalent. The calculated structural properties of $(ZnS)_{12}$, $(CdS)_{12}$, and $(CdSe)_{12}$ are in

DOI: 10.1021/acs.jpcc.5b08084
J. Phys. Chem. C 2015, 119, 25965−25973

good agreement with the previously reported values based on the same level of theory.[36,37] Analysis of Mulliken charges finds the chemical bonds to be mainly ionic in these semiconducting QDs.

The cagelike subnano QD was considered to approach the nucleobases toward all possible binding sites including ring nitrogen atom (i.e., the -N site, -NH site, and -N1 site), oxygen atom (i.e., O site), and center of hexagonal or pentagonal rings (i.e., top site) of the molecules. Some of the representative binding sites for uracil and adenine are shown in Figure 2. For the bioconjugated complex, we take the equilibrium configuration to be the minimum-energy configuration on the energy surface of a $(MX)_{12}$ approaching the target binding site of a nucleobase (an example is shown in Supporting Information Figure S1). The paths approaching the -N, -NH, -N1, and O sites were constrained in the plane of the base molecule while the path going to the top site was constrained perpendicular to the plane of the molecule.[39]

The chalcogenide QD is oriented in such a way that either metal-terminated or S/Se-terminated surface of the cluster interacts with the target binding-sites of the nucleobases. We find that the interaction of the S/Se-terminated surface of the cluster with the nucleobase molecules is not bound. This preference for the metal site is clearly demonstrated by the electrostatic potential plot, taking $(ZnS)_{12}$ interacting with cytosine as an example. The O or N site of cytosine is a highly electronegative center, which interacts with the Zn sites, the blue spots pertaining to positive potentials in the figure, while the greenish-yellow spots are S sites. A similar trend was found in the study of the adsorption of RNA/DNA nucleobases on the external surfaces of Na^+-montmorillonite, where the side comprising the Na^+ counterions interacts more strongly with two basic centers (N and O) of nucleobases than the opposite side, where only siloxane bonds are present.[23] Examples of interaction of nucleobases approaching the metal-terminated surface of the clusters from different binding sites are plotted in Figure 3.

The binding energy of the bioconjugated complex is defined via the asymptotic approach taking the difference in the total energies of the conjugated system at the equilibrium configuration and when they are far apart from each other (≈7 Å) (see Figure S1). The calculated results in gas phase show strong interaction from the O and N (or N1) sites of the nucleobases as plotted in Figure 4 (see a full summary of results in Table S2). We also find that the oxygen site is preferred over the nitrogen site when both exist in the case of cytosine and guanine. There appears to be no binding between the nucleobases and the semiconducting cluster via either top site or -NH site. Overall, the order of the interaction strength of the nucleobases with the $(MX)_{12}$ cluster is predicted to be C > G > T ∼ U for the oxygen site. For the given molecule, the binding energy of the complex decreases as we go from $(ZnS)_{12}$ to $(CdS)_{12}$ to $(CdSe)_{12}$. This is consistent with the basicity of the cation in the subnano QDs considered.

The most noticeable result comes out to be the solvent effect on the predicted stability of the complexes involving the chalcogenide QDs and nucleobases. The binding energies associated with the equilibrium configurations of bioconjugated complexes in water are plotted in the bottom panels of Figure 4a,b (see a full summary of results in Table S3). The calculated binding energy for the bioconjugate in gas phase is significantly higher than that calculated in the presence of the solvent water. Furthermore, the N site for most base molecules appears to be

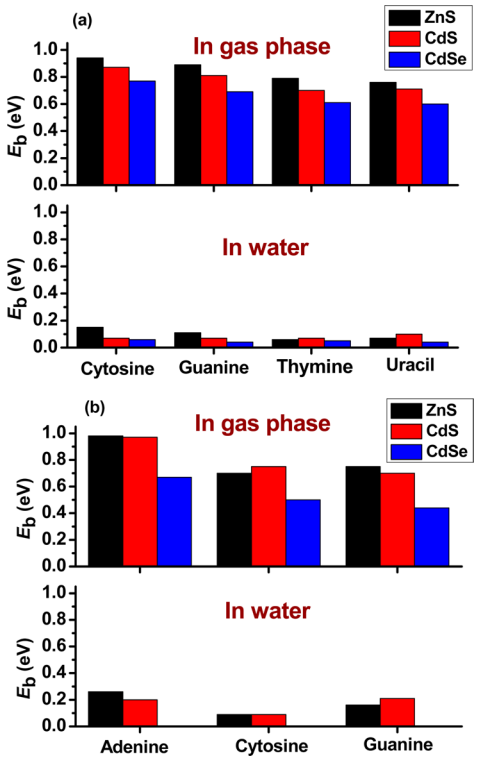

Figure 4. Calculated binding energies (E_b) of QD (modeled by $(ZnS)_{12}$, $(CdS)_{12}$, or $(CdSe)_{12}$ nanoclusters) bioconjugated complexes in gas phase and in water bound to nucleobases from (a) the O site and (b) the N site.

preferred over the oxygen site of the molecules in terms of the binding energy of the complex in the solution phase. In other words, the bioconjugated complexes binding at the N site are less affected by the presence of the aqueous medium.

The reason for the dramatic solvent effect can be attributed to the dominant electrostatic interaction between QDs and DNA bases, owing to the large differences in their values of electronegativity between Zn (1.65) or Cd (1.69) with O (3.44) or N (3.04). The Coulomb interaction between positively charged centers and negatively charged centers is the major contribution to the binding energy. In the presence of a dielectric medium, like water, the Coulomb interaction is reduced by a factor of the dielectric constant. Water is a strong polar molecule and has a relatively high dielectric constant (78.39). The effective binding energy, therefore, decreases due to the electrostatic screening. In addition, the electronegativity of N is smaller than that of O, which makes the polarity of the metal−N bond less than that of the metal−O bond. As a result of the increased covalency of the metal−N bond, the binding strength is less affected by the electrostatic screening.

This is also reflected in the analysis of the molecular orbitals. For instance, we plotted the highest occupied molecular orbitals (HOMOs) of the two lowest-energy bioconjugated complexes formed by $(ZnS)_{12}$ and a cytosine base binding at the O site and the N site in Figure 5.

In gas phase, the wave function spreads over the S-3p orbitals of $(ZnS)_{12}$ and the orbitals of the cytosine base composed of O-2p, N-2p for binding at the O site and O-2p, N-2p, C-2p for binding at the N site. Note that there is barely any contribution from the metal Zn cations in HOMO, while the states of Zn form the lowest unoccupied molecular orbitals (LUMOs). This is a clear indication of electrostatic interaction. Pronounced

DOI: 10.1021/acs.jpcc.5b08084
J. Phys. Chem. C 2015, 119, 25965−25973

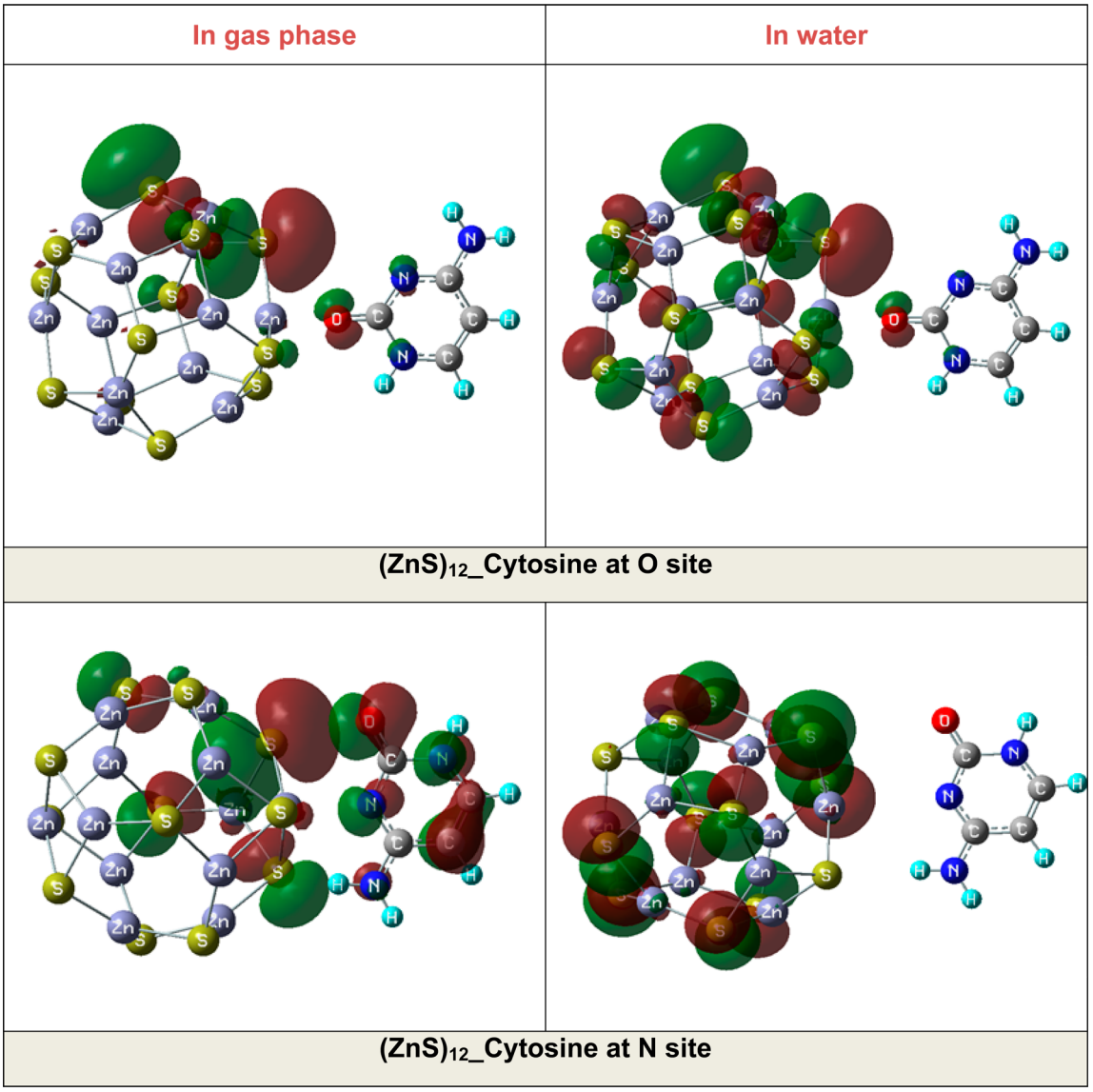

Figure 5. HOMOs of the bioconjugated complexes formed by a $(ZnS)_{12}$ nanocluster and a cytosine base at the O site (upper panel) and the N site (lower panel) in gas phase and in water.

change is observed for the HOMO going from the gas phase to the water solution. In water, the wave function is primarily located on $(ZnS)_{12}$ and distributed over S-3p orbitals.

BNNTs and DNA Oligomers. A finite cluster of $B_{66}N_{66}H_{12}$ is chosen to simulate the zigzag (6, 0) single-walled BN nanotube (BNNT) with a diameter of 0.5 nm. The cluster was cleaved from a BNNT, and the edge atoms with dangling bonds were passivated with H atoms. A fragment of homo-oligomers of DNA, namely 3A, 3C, 3G, and 3T, are considered for calculations. The effects of the phosphate group were neutralized by H atoms, thus simulating screening of the negative charge of the phosphate group by counterions in solution. The size of the cluster (~2.2 nm) is sufficiently large enough to allow all the possible interaction sites of BNNT with the DNA oligomer considered.

The DNA oligomers were fully relaxed, and the optimized structures are shown in Figure S2. It is observed that these free-standing structures tend to bend toward each other to form H-bonds in gas phase, while the structures are more extended in solution due to its polar nature. A number of orientations of these oligomers at different sites on BNNT were considered in order to determine the equilibrium configuration for the bioconjugated complex. BNNTs have four typical binding sites: the atop site of B, the atop site of N, the bridge site between B and N, and the hole site above the BN hexagon ring. There exist two distinct orientations, namely parallel and perpendicular orientations of the biomolecule with respect to the hexagonal rings of BNNT. In the parallel configuration, the molecules orientate parallel to the BNNT surface, maximizing the so-called $\pi-\pi$ interactions. In the perpendicular configuration, the molecules orientate perpendicular to the BNNT surface, and it is featured more of chemical bonding interacting through the O, N, or NH groups on the edge of nucleobases and the functional groups from the phosphate sugar backbone. The former is known to dominate for the case of carbon nanotubes, due to the highly saturated sp^2 bonding of hexagon carbon rings (honeycomb structure).[17] This, however, may not be fully the case for BN nanotubes due to the nonequal electronegativity of B and N atoms. After forming 3-fold bonding with each other, the B atom has an unoccupied p

DOI: 10.1021/acs.jpcc.5b08084
J. Phys. Chem. C 2015, 119, 25965−25973

orbital, while the N atom has a lone pair of electrons. Therefore, in general, this indicates a strong tendency for reactions with other elements. It is worth noting that there might be cases that in one DNA oligomer some base is parallel to the BNNT surface rings, while the other base is perpendicular to the BNNT surface. It is really an energetic competition among different orientations of different bases, also taking into account of the curvature of the considered BNNT. In order to further isolate the fundamental effects, calculations were performed with a single base cytosine to compare the parallel and the perpendicular orientation of base with respect to BNNT. The perpendicular orientation consistently shows a higher binding strength (by 0.7 eV) with BNNT than the parallel orientation (Figure S3). This preference is correlated with the relatively high polarizability of the (6,0) BNNT due to its large curvature.[40]

The equilibrium configuration of one of the DNA oligomers, 3C, is shown in Figure 6. A full list of results can be found in

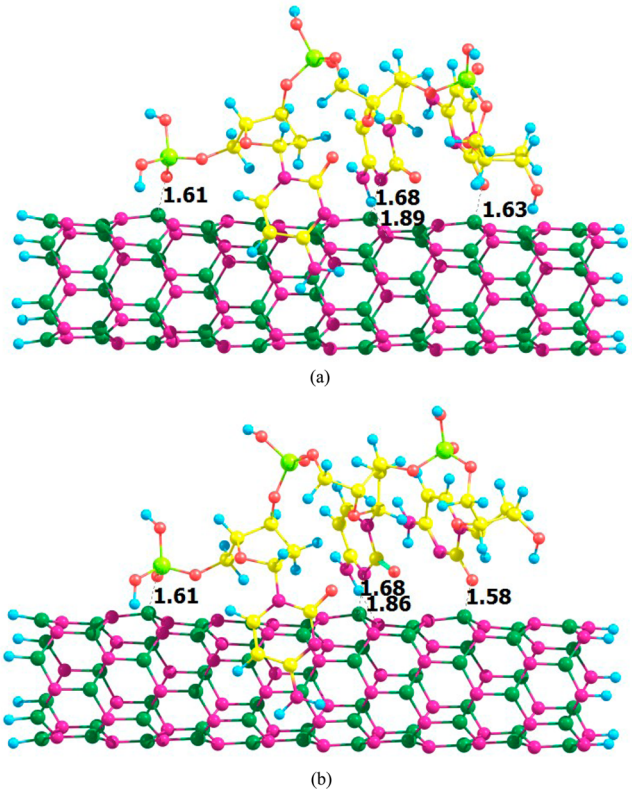

Figure 6. Binding configurations of a DNA oligomer 3C with a (6,0) BNNT in (a) gas phase and (b) water. Multiple binding sites exist with their distances labeled in the figures. Atoms are represented as C in yellow, N in magenta, H in light blue, O in red, P in light green, and B in dark green.

Figures S4 and S5. The binding energies are plotted in Figure 7. In contrast to the case of chalcogenide QDs interaction with nucleobases, two things stand out. First, the interactions are stronger for both in gas phase and in water. Second, the binding energies are fairly close for gas phase and water. In other words, there is barely any countereffect from the polar solvent of water for the BNNT interaction with DNA oligomers. It is worth mentioning that in the current study the solvent effects are taken into account implicitly with a continuum solvation model. The contribution from explicit water molecules is not

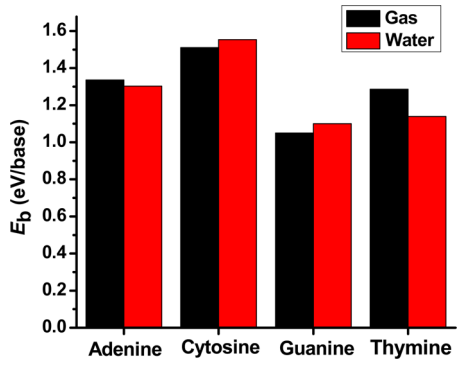

Figure 7. Calculated binding energies (E_b) of (6, 0) BNNT-DNA oligomer bioconjugated complexes in gas phase and in water. E_b is given per DNA base.

considered. Since water itself is a polar molecule having electronegative oxygen, the binding energy of a single water molecule could go up to a few tenths of an electronvolt.[41] It could potentially compete with nucleobases for the adsorption on BNNT surface.

Figure 7 shows 3C has the strongest interaction strength with BNNT, followed by 3A and 3T, while 3G has the lowest binding energy with BNNT. The order of interaction strength is in big contrast to the case of single DNA bases interaction with CNT[17,42] and BNNT[18] where the strongest interaction falls on guanine in a parallel stacking configuration, owing to the strong polarizability of guanine. In the case of BNNT interaction with DNA oligomers, the major interaction comes from the covalent bonding between BNNT and DNA oligomers, which we would rather call a perpendicular configuration. The six- or five-member rings of purines and pyrimidines lose their dominant role for forming a $\pi-\pi$ stacking[18] with the BN rings. Instead, the strong interaction comes from the edge of the nucleobases, which is usually featured by high-electronegative elements O, N and H-bond forming units of NH. For instance, in the case of 3C, there are primarily four binding sites (Figure 6): O(cytosine)−B(BN) with a distance of 1.58/1.63 Å (gas/aqueous); N(cytosine)−B(BN) with a distance of 1.68/1.68 Å (gas/aqueous); O(backbone)−B(BN) with a distance of 1.61/1.61 Å (gas/aqueous); NH(cytosine)···N(BN) with a distance of 1.89/1.86 Å (gas/aqueous) forming a H-bond. This can be understood by the local sp^3 hybridization of a B atom at the absorption site. A deformation from an in-plane triangular BO_3 to a tetrahedral BO_4 occurs. Boron is known to have both 3-fold and 4-fold coordination,[43] and B−O is a strong hybridized chemical bond with the 4-fold slightly weaker than the 3-fold. This is understandable from the difference in the electronegativity of B (2.04) and O (3.44), which is large enough to have a polar bond but small enough to maintain high covalency as compared to Zn (1.65) or Cd (1.69) with O (3.44) or N (3.04). In the electrostatic potential plots (Figure S6), B and N sites of BNNT have less visual contrast as compared to the chalcogenide clusters due to the smaller difference in their electronegativity. The blue B spots having positive potential tend to form bonds with the O and N sites of DNA pertaining negative potentials.

It is worth noting that there are multiple binding sites between the DNA oligomer and the BNNT. It demonstrates a mixture of parallel and perpendicular binding in the case of guanine and adenine—the purines. But the primary contribu-

DOI: 10.1021/acs.jpcc.5b08084
J. Phys. Chem. C 2015, 119, 25965−25973

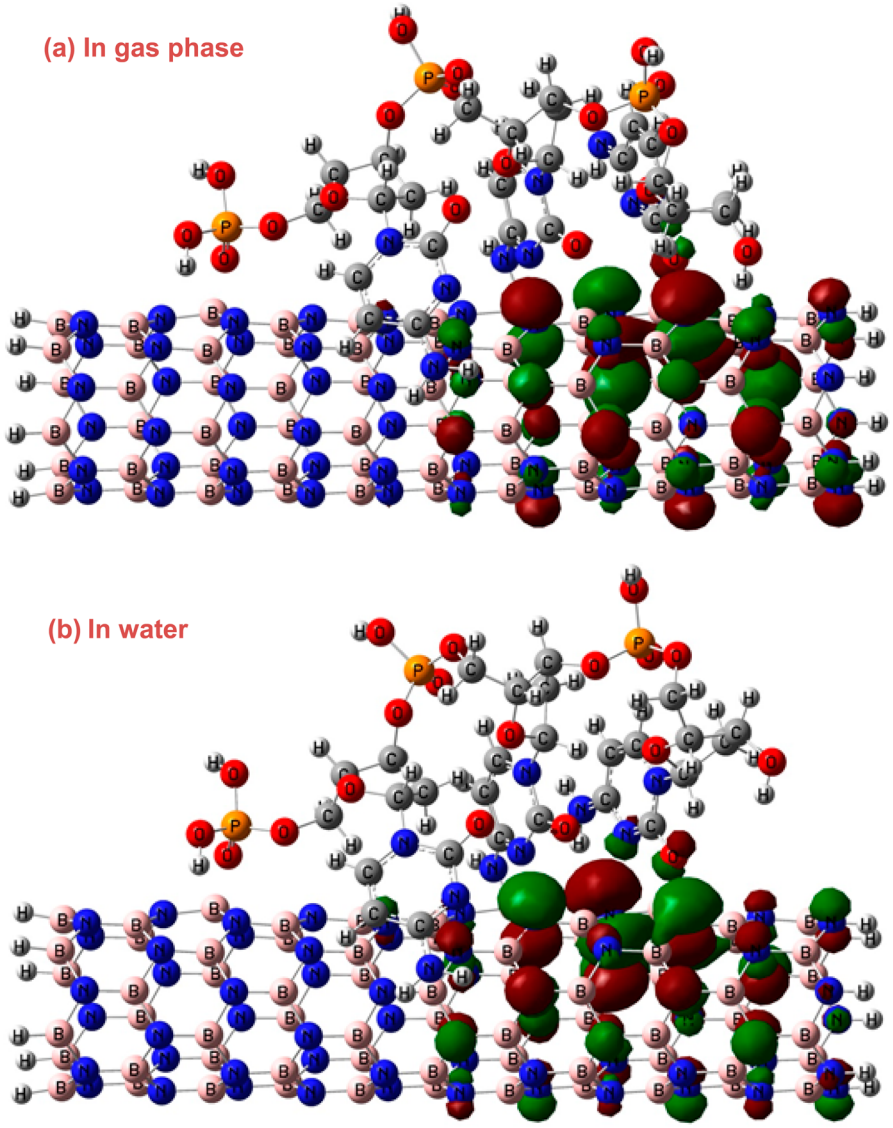

Figure 8. HOMOs of the bioconjugated complexes formed by BNNT and a DNA oligomer 3-cytosine (a) in gas phase and (b) in water.

tions are still from the perpendicular binding, where the DNA base stands relatively straight with BNNT and form direct chemical bonds. The parallel binding, on the other hand, is only seen when there is a favored orientation to have $\pi-\pi$ stacking of the rings of DNA with hexagonal BN rings.

The strong covalent interaction of BNNTs with organic molecules was previously observed in experiments for polymers and proteins[14,16] and reported for small polar molecules interacting with BNNTs from theoretical studies.[44] In addition, people have used covalent functionalization of the nanotube sidewalls in biomedical applications due to its high stability[45] and in electronics to modify BNNT electronic structures.[46]

The comparable binding configuration and energies found for the BNNT bioconjugates in both gas and aqueous phases are owing to the strong covalent bonding between BNNT and DNA. The HOMOs of the BNNT-3C bioconjugated complexes in gas phase and in water are plotted in Figure 8. Despite the primary contribution of N-2p states on the BNNT side, a strong hybridization of the B-2s2p states with the O-2p states of the DNA oligomer 3C at one of the binding sites is observed. And in contrast to the chalcogenide QDs interacting with DNA bases, the molecular orbitals of BNNT with 3C in gas phase and in water are very similar. Thus, with the shared electrons between the atoms forming a high-covalency bond, it is less perturbed by the existence of the polar solvent.

4. CONCLUSIONS

The chalcogenide QDs represented by the subnanometer $(ZnS)_{12}$, $(CdS)_{12}$, and $(CdSe)_{12}$ clusters interact strongly at their metal centers Zn or Cd featuring electrostatic interaction with the O or N site of DNA bases, while the BNNTs form covalent bonds with DNA oligomers at multiple B and/or N sites. The average binding energy per DNA base is higher for BNNTs than QDs. In both cases, cytosine shows the strongest binding strength. Most extraordinarily, the solvent effect is distinctively different for these two cases. The chalcogenide QDs have positively charged sites (the metal ions) which interact with available complementary electronegative sites on the nucleobase molecules. It is understandable that the dipole nature of water (the solvent modeled) competes with and significantly dampens this interaction. Thus, for such cases, it is imperative to include solvent effects in the modeling in order to capture this behavior which then properly scales the quantities

DOI: 10.1021/acs.jpcc.5b08084
J. Phys. Chem. C 2015, 119, 25965−25973

of interest (such as binding energies); that is, a solvent effect is required in order to properly set the scale of interaction in a solvent (water) environment when the solvent should clearly play a role in the interaction. For the BNNT interaction with DNA in water, the water does not "compete with" or play much (or any) role in the interaction. This interaction is then well represented by a straightforward gas phase model. It is, however, injudicious to generalize our results to interactions of BNNTs with other organic molecules because the nature of bonding could vary.[26] This study clearly demonstrates the different responses of electrostatic interaction vs covalent bonding in polar solvent and signifying the importance in performing the realistic simulation of the bioconjugated complexes. In addition, advancing theories of how a solvent medium influences chemical interactions can provide direct guidance for applications in materials science, catalysis, and biochemistry.

■ ASSOCIATED CONTENT

Supporting Information

The Supporting Information is available free of charge on the ACS Publications website at DOI: 10.1021/acs.jpcc.5b08084.

Summary of all binding energies and configurations of semiconducting nanostructure bioconjugated complexes with different binding sites and binding configurations in gas phase and in water; comparison of results at different levels of theory; calculation of the potential energy surface; painted electrostatic potential plots for a selection of representative bioconjugates (PDF)

■ AUTHOR INFORMATION

Corresponding Authors

*E-mail haiying.he@valpo.edu (H.H.).
*E-mail pandey@mtu.edu (R.P.).
*E-mail shashi.p.karna.civ@mail.mil (S.P.K.).

Notes

The authors declare no competing financial interest.

■ ACKNOWLEDGMENTS

The "Michigan Nano Computational Cluster" (MNC2) at University of Michigan was used in obtaining part of the results presented in this paper. We thank Dr. Behrouz Shiari at MNC2 for technical support. Helpful discussions with Dr. Saikat Mukhopadhyay and Dr. S. Gowtham are gratefully acknowledged.

■ REFERENCES

(1) Wang, L. Y.; Kan, X. W.; Zhang, M. C.; Zhu, C. Q.; Wang, L. Fluorescence for the Determination of Protein with Functionalized Nano-ZnS. *Analyst* **2002**, *127*, 1531−1534.

(2) Kloepfer, J. A.; Mielke, R. E.; Nadeau, J. L. Uptake of CdSe and CdSe/ZnS Quantum Dots into Bacteria via Purine-Dependent Mechanisms. *Appl. Environ. Microb* **2005**, *71*, 2548−2557.

(3) Kloepfer, J. A.; Bradforth, S. E.; Nadeau, J. L. Photophysical Properties of Biologically Compatible CdSe Quantum Dot Structures. *J. Phys. Chem. B* **2005**, *109*, 9996−10003.

(4) Pardo-Yissar, V.; Katz, E.; Wasserman, J.; Willner, I. Acetylcholine Esterase-Labeled US Nanoparticles on Electrodes: Photoelectrochemical Sensing of the Enzyme Inhibitors. *J. Am. Chem. Soc.* **2003**, *125*, 622−623.

(5) Wang, X. H.; Du, Y. M.; Ding, S.; Wang, Q. Q.; Xiong, G. G.; Xie, M.; Shen, X. C.; Pang, D. W. Preparation and Third-Order Optical Nonlinearity of Self-Assembled Chitosan/CdSe-ZnS Core-Shell Quantum Dots Films. *J. Phys. Chem. B* **2006**, *110*, 1566−1570.

(6) Rubio, A.; Corkill, J. L.; Cohen, M. L. Theory of Graphitic Boron-Nitride Nanotubes. *Phys. Rev. B: Condens. Matter Mater. Phys.* **1994**, *49*, 5081−5084.

(7) Chopra, N. G.; Luyken, R. J.; Cherrey, K.; Crespi, V. H.; Cohen, M. L.; Louie, S. G.; Zettl, A. Boron-Nitride Nanotubes. *Science* **1995**, *269*, 966−967.

(8) Terrones, M.; Romo-Herrera, J. M.; Cruz-Silva, E.; Lopez-Urias, F.; Munoz-Sandoval, E.; Velazquez-Salazar, J. J.; Terrones, H.; Bando, Y.; Golberg, D. Pure and Doped Boron Nitride Nanotubes. *Mater. Today* **2007**, *10*, 30−38.

(9) Li, X.; Zhi, C.; Hanagata, N.; Yamaguchi, M.; Bando, Y.; Golberg, D. Boron Nitride Nanotubes Functionalized with Mesoporous Silica for Intracellular Delivery of Chemotherapy Drug. *Chem. Commun.* **2013**, *49*, 7337−7339.

(10) Lahiri, D.; Rouzaud, F.; Richard, T.; Keshri, A. K.; Bakshi, S. R.; Kos, L.; Agarwal, A. Boron Nitride Nanotube Reinforced Polylactide-Polycaprolactone Copolymer Composite: Mechanical Properties and Cytocompatibility with Osteoblasts and Macrophages in Vitro. *Acta Biomater.* **2010**, *6*, 3524−3533.

(11) Ciofani, G.; Danti, S.; D'Alessandro, D.; Ricotti, L.; Moscato, S.; Bertoni, G.; Falqui, A.; Berrettini, S.; Petrini, M.; Mattoli, V.; Menciassi, A. Enhancement of Neurite Outgrowth in Neuronal-Like Cells following Boron Nitride Nanotube-Mediated Stimulation. *ACS Nano* **2010**, *4*, 6267−6277.

(12) Maria Nithya, J. S.; Pandurangan, A. Aqueous Dispersion of Polymer Coated Boron Nitride Nanotubes and their Antibacterial and Cytotoxicity Studies. *RSC Adv.* **2014**, *4*, 32031−32046.

(13) Ciofani, G.; Raffa, V.; Menciassi, A.; Cuschieri, A. Cytocompatibility, Interactions, and Uptake of Polyethyleneimine-Coated Boron Nitride Nanotubes by Living Cells: Confirmation of Their Potential for Biomedical Applications. *Biotechnol. Bioeng.* **2008**, *101*, 850−858.

(14) Zhi, C.; Bando, Y.; Tang, C.; Golberg, D. Immobilization of Proteins on Boron Nitride Nanotubes. *J. Am. Chem. Soc.* **2005**, *127*, 17144−17145.

(15) Zhi, C.; Bando, Y.; Wang, W.; Tang, C.; Kuwahara, H.; Golberg, D. DNA-Mediated Assembly of Boron Nitride Nanotubes. *Chem. - Asian J.* **2007**, *2*, 1581−1585.

(16) Zhi, C. Y.; Bando, Y.; Tang, C. C.; Honda, S.; Sato, K.; Kuwahara, H.; Golberg, D. Characteristics of Boron Nitride Nanotube-Polyaniline Composites. *Angew. Chem., Int. Ed.* **2005**, *44*, 7929−7932.

(17) Gowtham, S.; Scheicher, R. H.; Pandey, R.; Karna, S. P.; Ahuja, R. First-Principles Study of Physisorption of Nucleic Acid Bases on Small-Diameter Carbon Nanotubes. *Nanotechnology* **2008**, *19*, 125701.

(18) Mukhopadhyay, S.; Gowtham, S.; Scheicher, R. H.; Pandey, R.; Karna, S. P. Theoretical Study of Physisorption of Nucleobases on Boron Nitride Nanotubes: a New Class of Hybrid Nano-Biomaterials. *Nanotechnology* **2010**, *21*, 165703.

(19) Lin, Q.; Zou, X.; Zhou, G.; Liu, R.; Wu, J.; Li, J.; Duan, W. Adsorption of DNA/RNA Nucleobases on Hexagonal Boron Nitride Sheet: an ab initio Study. *Phys. Chem. Chem. Phys.* **2011**, *13*, 12225−12230.

(20) Shukla, M. K.; Dubey, M.; Zakar, E.; Leszczynski, J. DFT Investigation of the Interaction of Gold Nanoclusters with Nucleic Acid Base Guanine and the Watson−Crick Guanine-Cytosine Base Pair. *J. Phys. Chem. C* **2009**, *113*, 3960−3966.

(21) Soto-Verdugo, V.; Metiu, H.; Gwinn, E. The properties of Small Ag Clusters Bound to DNA Bases. *J. Chem. Phys.* **2010**, *132*, 195102.

(22) Saha, S.; Sarkar, P. Understanding the Interaction of DNA-RNA Nucleobases with Different ZnO Nanomaterials. *Phys. Chem. Chem. Phys.* **2014**, *16*, 15355−15366.

(23) Mignon, P.; Ugliengo, P.; Sodupe, M. Theoretical Study of the Adsorption of RNA/DNA Bases on the External Surfaces of Na +-Montmorillonite. *J. Phys. Chem. C* **2009**, *113*, 13741−13749.

(24) Mignon, P.; Sodupe, M. Theoretical Study of the Adsorption of DNA Bases on the Acidic External Surface of Montmorillonite. *Phys. Chem. Chem. Phys.* **2012**, *14*, 945−954.

DOI: 10.1021/acs.jpcc.5b08084
J. Phys. Chem. C 2015, 119, 25965−25973

(25) Rimola, A.; Sodupe, M. Gas-Phase and Microsolvated Glycine Interacting with Boron Nitride Nanotubes. A B3LYP-D2* Periodic Study. *Inorganics* **2014**, *2*, 334.
(26) Farmanzadeh, D.; Ghazanfary, S. DFT Studies of Functionalized Zigzag and Armchair Boron Nitride Nanotubes as Nanovectors for Drug Delivery of Collagen Amino Acids. *Struct. Chem.* **2014**, *25*, 293−300.
(27) Frisch, M. J.; Trucks, G. W.; Schlegel, H. B.; Scuseria, G. E.; Robb, M. A.; Cheeseman, J. R.; Montgomery, J. A., Jr.; Vreven, T.; Kudin, K. N.; Burant, J. C.; et al. *GAUSSIAN09*; Gaussian: Pittsburgh, PA, 2009.
(28) Lee, C. T.; Yang, W. T.; Parr, R. G. Development of the Colle-Salvetti Correlation-Energy Formula into a Functional of the Electron-Density. *Phys. Rev. B: Condens. Matter Mater. Phys.* **1988**, *37*, 785−789.
(29) Hay, P. J.; Wadt, W. R. Ab initio Effective Core Potentials for Molecular Calculations - Potentials for K to Au Including the Outermost Core Orbitals. *J. Chem. Phys.* **1985**, *82*, 299−310.
(30) Wadt, W. R.; Hay, P. J. Abinitio Effective Core Potentials for Molecular Calculations - Potentials for Main Group Elements Na to Bi. *J. Chem. Phys.* **1985**, *82*, 284−298.
(31) Dunning Jr., T. H.; Hay, P. J. In *Modern Theoretical Chemistry*; Schaefer III, H. F., Ed.; Plenum: New York, 1977; Vol. 3, pp 1−28.
(32) Grimme, S. Semiempirical GGA-type Density Functional Constructed with a Long-Range Dispersion Correction. *J. Comput. Chem.* **2006**, *27*, 1787−1799.
(33) Chai, J. D.; Head-Gordon, M. Long-Range Corrected Hybrid Density Functionals with Damped Atom-Atom Dispersion Corrections. *Phys. Chem. Chem. Phys.* **2008**, *10*, 6615−6620.
(34) Chai, J. D.; Head-Gordon, M. Systematic Optimization of Long-Range Corrected Hybrid Density Functionals. *J. Chem. Phys.* **2008**, *128*, 084106.
(35) Tomasi, J.; Mennucci, B.; Cammi, R. Quantum Mechanical Continuum Solvation Models. *Chem. Rev.* **2005**, *105*, 2999−3093.
(36) Burnin, A.; Sanville, E.; BelBruno, J. J. Experimental and Computational Study of the Zn_nSn and Zn_nSn+ Clusters. *J. Phys. Chem. A* **2005**, *109*, 5026−5034.
(37) Sanville, E.; Burnin, A.; BelBruno, J. J. Experimental and Computational study of Small (n = 1−16) Stoichiometric Zinc and Cadmium Chalcogenide Clusters. *J. Phys. Chem. A* **2006**, *110*, 2378−2386.
(38) Wang, B. L.; Wang, X. Q.; Chen, G. B.; Nagase, S. G.; Zhao, J. J. Cage and Tube Structures of Medium-Sized Zinc Oxide Clusters (ZnO)(n) (n = 24, 28, 36, and 48). *J. Chem. Phys.* **2008**, *128*, 144710.
(39) Shewale, V.; Joshi, P.; Mukhopadhyay, S.; Deshpande, M.; Pandey, R.; Hussain, S.; Karna, S. P. First-Principles Study of Nanoparticle-Biomolecular Interactions: Anchoring of a (ZnO)(12) Cluster on Nucleobases. *J. Phys. Chem. C* **2011**, *115*, 10426−10430.
(40) Kryachko, E. S.; Remacle, F. Complexes of DNA Bases and Watson−Crick Base Pairs with Small Neutral Gold Clusters. *J. Phys. Chem. B* **2005**, *109*, 22746−22757.
(41) Rimola, A.; Sodupe, M. Physisorption vs. Chemisorption of Probe Molecules on Boron Nitride Nanomaterials: the Effect of Surface Curvature. *Phys. Chem. Chem. Phys.* **2013**, *15*, 13190−13198.
(42) Gowtham, S.; Scheicher, R. H.; Ahuja, R.; Pandey, R.; Karna, S. P. Physisorption of Nucleobases on Graphene: Density-Functional Calculations. *Phys. Rev. B: Condens. Matter Mater. Phys.* **2007**, *76*, 033401.
(43) Sauer, H.; Brydson, R.; Rowley, P. N.; Engel, W.; Thomas, J. M. Determination of Coordinations and Coordination-Specific Site Occupancies by Electron Energy-Loss Spectroscopy - an Investigation of Boron Oxygen Compounds. *Ultramicroscopy* **1993**, *49*, 198−209.
(44) Ganji, M.; Rezvani, M. Boron Nitride Nanotube Based Nanosensor for Acetone Adsorption: a DFT Simulation. *J. Mol. Model.* **2013**, *19*, 1259−1265.
(45) Zhang, H. J.; Chen, S.; Zhi, C. Y.; Yamazaki, T.; Hanagata, N. Chitosan-Coated Boron Nitride Nanospheres Enhance Delivery of CpG Oligodeoxynucleotides and Induction of Cytokines. *Int. J. Nanomed.* **2013**, *8*, 1783−1793.
(46) Zhi, C. Y.; Bando, Y.; Tang, C. C.; Golberg, D. Engineering of Electronic Structure of Boron-Nitride Nanotubes by Covalent Functionalization. *Phys. Rev. B: Condens. Matter Mater. Phys.* **2006**, *74*, 153413.

DOI: 10.1021/acs.jpcc.5b08084
J. Phys. Chem. C 2015, 119, 25965−25973